frontiers | Frontiers in Earth Science

REVIEW
published: 12 July 2022
doi: 10.3389/feart.2022.930474

Microstructure Characterization Techniques for Shale Reservoirs: A Review

Yujing Qian[1,2], Ping Gao[1,2], Xianglong Fang[1,2], Fengrui Sun[1,2], Yidong Cai[1,2] and Yingfang Zhou[3]*

[1]School of Energy Resources, China University of Geosciences, Beijing, China, [2]Coal Reservoir Laboratory of National Engineering Research Center of CBM Development & Utilization, China University of Geosciences, Beijing, China, [3]School of Engineering, King's College, University of Aberdeen, Aberdeen, United Kingdom

The microstructure of shale reservoirs refers to the distribution of mineral–organic matter, pore–fracture features, diagenetic processes, and their interrelations. The comprehensive and accurate analysis of the shale microstructure plays a critical role in formulating a reasonable development plan and optimizing measures to enhance oil or gas recovery. To explore the microstructure characterization, the mineral and organic matter compositions as well as the pore types and distributions of organic-rich shale reservoirs were investigated using a series of advanced techniques, including focused ion beam–scanning electron microscopy and atomic force microscopy. This review establishes a model of pore distribution of the layered structure of shale reservoirs based on ideal shale laminae model. Among them, quartz and carbonate laminae can be classified as grain laminae clay minerals and organic matter and pyrite can be combined into organic matter aggregate due to the symbiotic relationship between pyrite, organic matter and clay minerals. Microcracks of diverse diagenetic origins can be classified together. This review also systematically summarizes the microcharacterization techniques and different characteristics of organic-rich shale reservoirs, thereby paving the way for the establishment of shale cross-scale characterization techniques.

Keywords: shale, microcharacterization, pore type, technology application, mineral

OPEN ACCESS

Edited by:
Yuqi Wu,
China University of Petroleum, China

Reviewed by:
Peng Cheng,
Guangzhou Institute of Geochemistry (CAS), China
Qin Zhou,
Guangzhou Institute of Geochemistry (CAS), China

****Correspondence:***
Ping Gao
gaoping1212@cugb.edu.cn

Specialty section:
This article was submitted to Solid Earth Geophysics, a section of the journal Frontiers in Earth Science

Received: *28 April 2022*
Accepted: *31 May 2022*
Published: *12 July 2022*

Citation:
Qian Y, Gao P, Fang X, Sun F, Cai Y and Zhou Y (2022) Microstructure Characterization Techniques for Shale Reservoirs: A Review. Front. Earth Sci. 10:930474. doi: 10.3389/feart.2022.930474

1 INTRODUCTION

In the past two decades, the increasing demand for energy and the accompanying energy has forced people to pay more attention to other energy sources that can replace conventional oil and gas. The exploration, production, and development of unconventional oil and gas resources, e.g., shale gas, have greatly solved the problem of human energy demand. Shale gas is natural gas stored in shale, which is traditionally considered to be the seal rock (Zou et al., 2015). With the characteristics of efficient development and environmental protection, shale gas has become an important strategic energy source for many countries around the world. The large-scale exploitation of shale gas helps alleviate the pressure of the energy supply. In order to reduce the dependence on foreign oil, China has experienced rapid development of shale gas reserves and development technology. By 2020, the annual output of shale gas was 200×10^8 m^3 in shallowly buried depths (<3,500 m), and major breakthroughs have also been made in the deep shale (burial depth of 3,500–4,000 m (Zou et al., 2021). The reservoir microstructure of organic-rich shale, which is composed of diagenetic minerals, organic matter, and pore

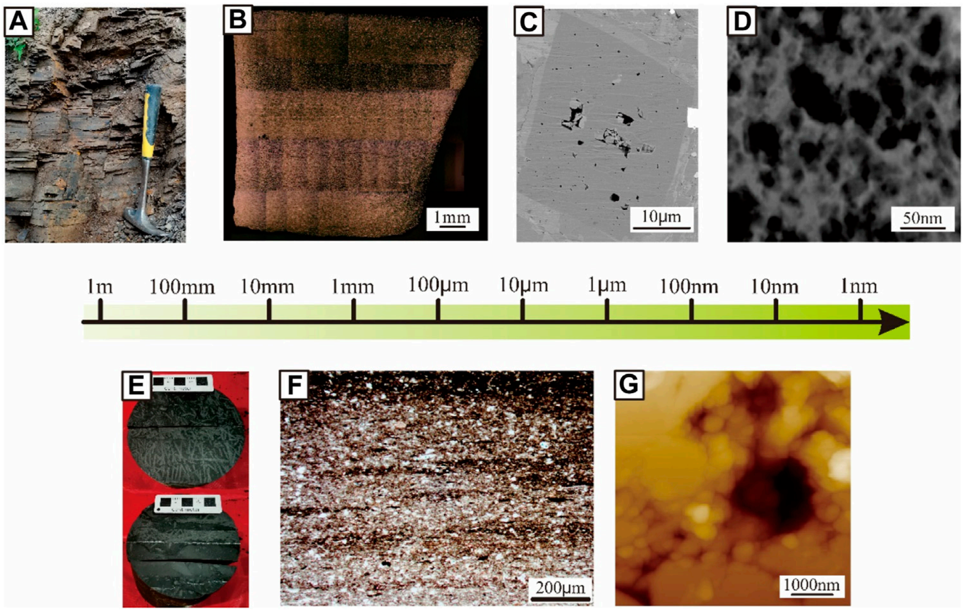

FIGURE 1 | Microscopic characteristics of shale at various scales. **(A)** XHY-1 shale outcrop of the Xiamaling Formation in the Zhangjiakou section; **(B)** Reflected light image of argon ion polished shale (PS1-2, Wufeng Formation, 5964.5 m); **(C)** FESEM image of argon ion polished shale (N228-14, Longmaxi Formation, 3,377.9 m); **(D)** Scanning transmission electron microscopy image of kerogen from the Barnett shale sample (Curtis et al., 2011); **(E)** Photos of shale cores of Longmaxi Formation in the Sichuan Basin (DY5-49, 3,811.5 m); **(F)** Single polarized light image of Longmaxi Formation shale in Yanjin (N228-1, 3,365.1 m); and **(G)** Atomic force microscopy images of micropores in polished shale (JY4-05, Wufeng Formation, 2,591.7 m).

network, is a key factor affecting the shale gas storage and seepage, thereby influencing shale gas enrichment and its yields.

With the increase in shale gas exploration, it has been found that there are great differences in the diagenetic minerals, organic matter, and pore network structure of different shales (Peltonen et al., 2009; Ross and Bustin, 2009; Xiao et al., 2015). The research methods mainly include scanning electron microscopy (SEM), mercury intrusion, and liquid nitrogen adsorption. However, the distribution of pores in shale reservoirs remains unclear, and a unified technical system and standard for the full-scale pore characterization are also lacking. Therefore, the purpose of this article is to 1) summarize the distribution of minerals, organic matter, and pore network structure; 2) conduct a comparative study on the evaluation methods of microscopic pore–fracture network structure of shale reservoirs; and 3) sort out the principles, scales, and characteristics of various testing methods. In addition, this review will provide a basis for the evaluation of shale reservoirs and the prediction of "sweet-spots," thereby providing a scientific support for shale gas exploration.

2 MICROSCOPIC CHARACTERISTICS OF SHALE RESERVOIRS

The practice of shale gas exploration shows that the gas production from shale with laminar structures is significantly different from that of conventional sandstone reservoir. From the field outcrop of the Xiamaling Formation, the shale generally exhibits gray bedding, and the thickness of a single layer is 0.5–10 cm. Fossils, mineral particles, and bedding in shale can be observed at a scale of 100 mm–100 μm. Pores in shale minerals and organic matter can be observed at the micro-nano scale, thereby showing the internal morphology of various pores (**Figure 1**). Numerous previous works have proved that the shale reservoirs display strong heterogeneity because of their bedding, and differences are found in mineral composition, organic matter distribution, and pore structure in laminated shale (Qiu and Zou, 2020; Sang et al., 2022).

As the most characteristic sedimentary feature in shale, laminar structure is an indispensable content in the basic research and exploration of unconventional oil sedimentology. In the study of laminae of marine shale and continental shale, researchers found that silty laminae demonstrate an important influence on the pore structure (Ross and Bustin, 2009; Lei et al., 2015). Many researchers have divided the Chang seven shales into bright and dark layers, and they pointed out that the contents of plagioclase and illite were the main difference between the bright and dark layers (Liu et al., 2016a; Liu et al., 2016b; Liu G. et al., 2021). Some authors have compared and evaluated the mineral compositions of argillaceous laminae and silty laminae in the Longmaxi Formation shale, and they pointed out that the contents of quartz and carbonate displayed the obvious differences (Shi et al., 2018; Liu et al., 2019a). For the pore structure of shale, researchers proposed that the development of laminae controls the size and pore-size distribution of inorganic macropores, which affects the pore structure and fracture formation of shale, and it is conducive to improving

TABLE 1 | The type of shale pores (Loucks et al., 2012).

Pore types of shale	
Interparticle pores	Pores between grains Pores between crystals Pores between clay platelets Pores at the edge of rigid grains
Intraparticle pores	Intercrystalline pores within pyrite framboids Pores within peloids or pellets Pores within fossil bodies Intraplatelet pores within clay platelets Moldic pores Dissolution-rim pores
Organic Matter pores	
Fracture pores	

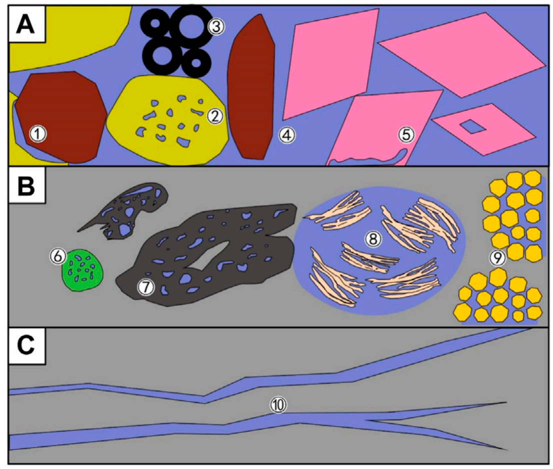

FIGURE 2 | Key components of shale microstructure and their relationships with pores. **(A)** Grain laminae: (1) pores at the edge of rigid grains, (2) moldic pores, (3) pores within fossil bodies, (4) pores between grains and crystals, and (5) dissolution-rim pores; **(B)** Organic-matter aggregates: (6) pores within peloids or pellets, (7) organic-matter pores, (8) pores between or within clay platelets, and (9) intercrystalline pores within pyrite framboids; and **(C)** (10) fracture.

the physical properties of the reservoir, especially the horizontal permeability (Li J. et al., 2015; Lai et al., 2018; Wu et al., 2019b; Wu et al., 2020a).

According to different sedimentary environments, shale can be divided into marine shale, transitional shale, and continental shale, all of which are ideal gas producing formations (Zou et al., 2017). These shales display different compositions of minerals and organic matter, and a series of measurement methods, such as X-ray diffraction, organic kerogen extraction, etc., could help us form a clear understanding of the components of shales. Generally speaking, laminae is a common feature indicating the sedimentary environment, which is also a constituent unit of minerals and organic matter. With the change in the sedimentary environment, the laminae usually contain different components, such as clay minerals, clastic minerals, such as quartz and feldspar, carbonate minerals, and organic matter (Ingram, 1954).

According to **Table 1**, pores in shale can be divided into interparticle pores, intraparticle pores, organic matter pores, and fracture according to different carriers (Loucks et al., 2012). Inspired by the laminar structure of shale (Ingram, 1954; Campbell, 1967; Lazar et al., 2015; Qiu and Zou, 2020; Yang et al., 2020), the shale can be simplified into a superimposed model of grain laminae, organic matter aggregate, and fracture (**Figure 2**). Grain laminae include carbonate and quartz-feldspar lamina, which are composed of quartz, feldspar, calcite, dolomite, etc. It can be found to be granular or crystalline under the microscope (**Figure 4**). Next, these laminae determine the brittleness of the shale and provide some stiffness to the overall structure of the rock. Organic matter aggregate is shale's important carrier of pore space. Organic matter, clay minerals, and pyrite are closely associated. Organic matter consists of kerogen and asphalt, which can be thermally cracked to be gas at the same time, thereby forming a large number of micro/nanoscaled pores. Organic matter is the parent material of hydrocarbon generation in shales and yields the important nanoscale reservoir spaces with increasing maturity. Clay minerals consist of kaolinite, chlorite, illite, and montmorillonite, which exhibit high plasticity, and under the condition of high maturity, will develop larger specific surface area of clay mineral contents of pore (Li C. et al., 2019) and store a certain amount of adsorbed gas and free gas. Next, the presence of pyrite indicates a reducing environment and often coexists with organic matter and clay. Due to its strong rigidity, intercrystalline pores may be found within pyrite framboids. Microfractures include bedding fractures, tectonic stress fractures, dissolution fractures, and contraction fractures of diagenetic dehydration/recrystallization, which are good hydrocarbon migration channels and an important part of the pore network.

Due to the existence of large number of micro-nano scale pores and fractures in shale, shale can become a natural gas reservoir; this has been proved by the practice of exploration and development at home and abroad. For shale gas reservoirs, micro/nanopores network can provide a storage space for free and adsorbed gases. On the other hand, the presence of numerous pores increases the specific surface area of the shale reservoir, thereby increasing the potential content of shale gas in the adsorbed state (Curtis, 2002). In addition, the existence of connected pores and fractures increases the seepage capacity of the reservoir to a certain extent, thereby facilitating the effective exploitation of shale gas. Therefore, the difficulty of microstructure research is the study of the spatial configuration of minerals, organic matter, and pores. The existing technology or system is only partially mature, and the splicing of scales and cross-scale research still need to be systematically improved and studied. The following is a brief introduction of several microstructural research methods focusing on pore space and mineral–organic matter associations.

3 TECHNIQUES FOR SHALE MICROSTRUCTURE CHARACTERIZATION

For the characterization of microscopic minerals, organic matter, and the pore–fracture network structure in shale reservoirs, the

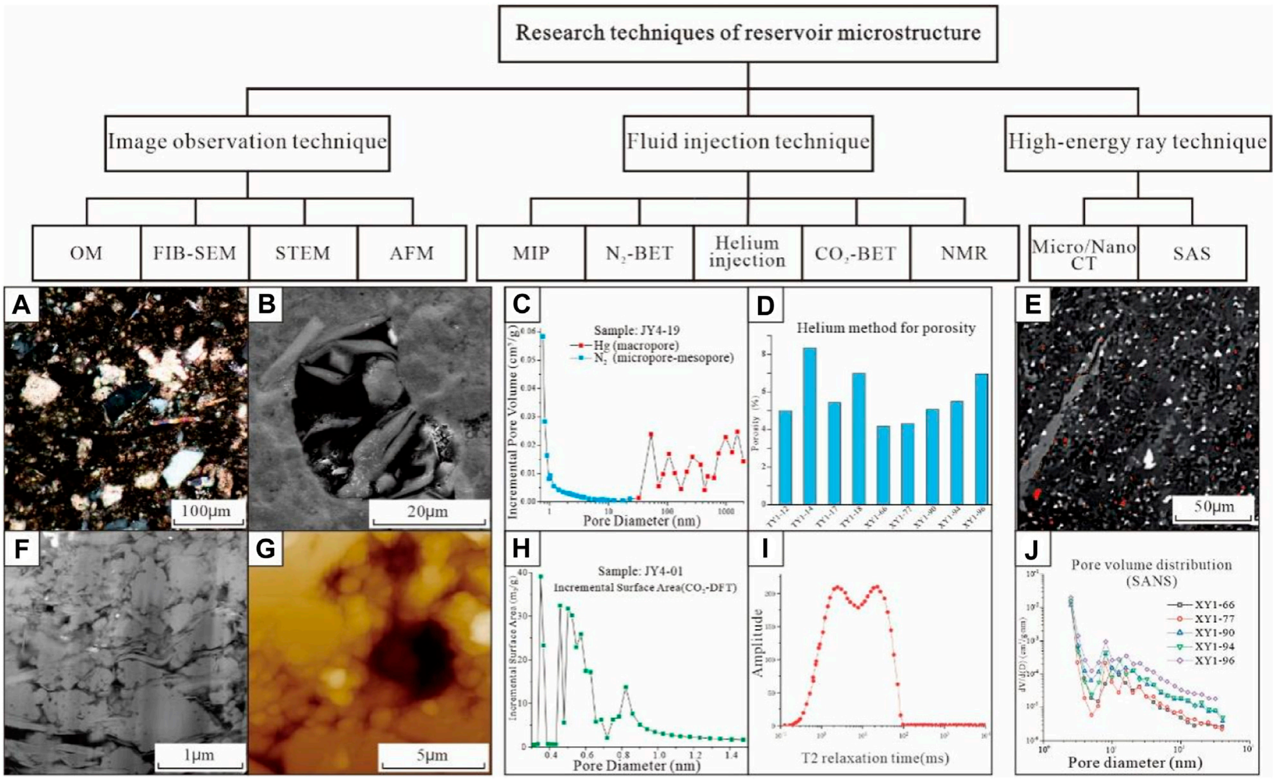

FIGURE 3 | Research method of reservoir microstructure. **(A)** Distribution of components in N228 shale under orthogonal polarization; **(B)** Focused ion beam–scanning electron microscopy images of pore fractures and minerals in XHY-1; **(C)** Characterization of shale pore distribution by mercury injection and nitrogen adsorption; **(D)** Porosity measured by helium injection; **(E)** Two-dimensional distribution of shale minerals and fractures under micro CT (Gou et al., 2019); **(F)** Shale dark field scanning transmission electron microscopy image (Peng et al., 2014); **(G)** JY4-05 (Wufeng Formation, 2591.7 m) shale surface topography under atomic force microscopy; **(H)** The surface area distribution of carbon dioxide adsorption; **(I)** Nuclear magnetic resonance of water-saturated shale (Sun et al., 2012); and **(J)** Shale pore volume distribution under small angle neutron scattering (Sun M. et al., 2017)).

techniques can be classified into three categories (**Figure 3**): image observation method, fluid injection method, and high-energy ray method. These methods for characterizing reservoir parameters exhibit certain differences. Image observation method focuses on direct observation, and resolution is the key. It is mainly used to study the size, morphology, and distribution of minerals, organic matter, and pores qualitatively. Next, the fluid injection method is an indirect measurement method, and the research scale is the key technology. It is mainly used to quantitatively analyze the size and distribution of the reservoir space. The high-energy ray method is also an indirect analysis method, and its repeatability is the key technology. Its advantage is that it can quantitatively analyze the shape, size, and distribution characteristics of closed pores and joints (**Table 2**).

3.1 Imaging Techniques and Microstructure Morphology

3.1.1 Advantage and Limitations

The image observation method mainly uses a microscope (optical microscopy, focused ion beam–SEM (FIB-SEM), atomic force microscopy (AFM), and scanning transmission electron microscopy (STEM)) to observe directly, and it carries out the statistical analysis of reservoir minerals, organic matter, and pores and fissures.

Optical microscopy is a direct observation of the thin reservoir pore structure, but the resolution is low: approximately 0.01 mm. It is mainly suitable for qualitative research on larger pores but cannot meet the needs of the observation of micro-nanopores in unconventional reservoirs. Although optical microscopy can exhibit a relatively comprehensive control of the sample, it can see the type and shape of inclusions in the thin section and then determine the gas generation stage of the target shale; at the same time, it can observe the mineral arrangement and morphological characteristics in the thin section to understand the diagenesis process. By observing the proportion and types of minerals in the reflected light mode (**Figure 4**), the source and genesis can be analyzed, but optical microscopy also exhibits the disadvantage of difficulty with quantitatively characterizing the size and connectivity of the reservoir space; thus, it needs to be used in combination with other methods.

The principle of FIB-SEM is to continuously cut the sample with a gallium ion beam and image it under the electron beam at the same time. Three-dimensional structural characteristics of shale nanopores are truly restored, and the analysis results of the three-dimensional spatial composition, pore-size distribution,

TABLE 2 | Techniques for shale microstructure characterization.

		Advantages	Disadvantages	Applicability	Limitation
Image observation technique	Optical microscope	A direct observation of the thin reservoir pore structure	The resolution is low: approximately 0.01 mm	It is mainly suitable for qualitative research on larger pores (> 0.01 mm)	It is difficult to quantitatively characterize the connectivity of the reservoir space
	FIB-SEM	Three-dimensional structural characteristics of shale are truly restored	Pores with diameters less than resolution or cutting spacing are not counted	It is suitable for studying the three-dimensional structure of nanoscale pores (>1 nm) in shales	The test does not count pores smaller than 10 nm in diameter, thereby making the experimental results smaller than the actual value
	STEM	It can characterize the three-dimensional nano structure of shale	The two-dimensional image contains both surface and interior information, which reduces the ability to characterize the pore structure of the shale surface	Suitable for the study of organic matter and mineral crystal structure (0.1 nm)	Very high requirements for sample preparation
	AFM	It can obtain the morphological features of the sample surface	Small imaging range and slow speed	It can be used to observe pore distribution (> 0.1 nm)	Very high requirements on the surface roughness of the sample
Fluid injection technique	MIP	High consistency between experimental results and physical property test results	It will destroy the sample and create artificial cracks	Describe reservoir pore-throat characteristics and seepage capacity	Experimental error exists in the measurement of pore throats with pore diameter less than 50 nm
	N2-BET	It can accurately characterize the pore volume and specific surface area of mesopores	The measurement error of rock samples with small contrast surface area is large	The test object is mesopore. Not suitable for measurement under high-temperature and high-pressure conditions	There is an error in measuring shales with a smaller specific surface area. It is not accurate enough to measure pores with pore sizes beyond 100 nm
	Helium injection	It can get the porosity parameter of connected pores	Only connected pores can be studied	It applies to the determination of porosity	It is difficult to reflect the pore-throat distribution
	CO_2-BET	The CO_2 can enter the pores with diameter of approximately 0.35 nm, which help calculate the micropore distribution in the sample	The particle size and water content of the sample affects the accuracy of the results	Mainly measures connected micropores with a pore size of 0.35–1.5 nm	May not harmonize sample handling standards and key experimental parameters
	NMR	Able to conduct research on pore distribution, oil–water distribution, and rock internal structure. The experiment process is fast, nondestructive, and intuitive	The experimental results are affected by many factors, such as the environment, instrument parameters, micropores of the sample, and fluid types	It can reflect the size, distribution, connectivity, and fluid occurrence characteristics of shale pores	The accuracy of the results is subject to the influence of test environment, fluid properties, and other factors
High-energy ray technique	Micro/ Nano-CT	It can characterize the three-dimensional structure of pores, which can be used to evaluate the connectivity of pores		It can present the three-dimensional spatial structure of pores and evaluate the connectivity of pores	The reliability of the reconstructed model needs to be verified after imaging
	SAS	1. The experimental results have high accuracy and repeatability 2. Will not destroy the sample 3. It can be combined with fluid injection method to obtain the structural characteristics of closed pores of shales	1.Expensive 2.The detection range is concentrated in the range of micropores and mesopores	It is suitable for closed pore research of shale	1. It is difficult to acquire synchrotron radiation machine 2. The pore structure interpretation model (SAS) of shale is not yet mature, which cannot explain the experimental results; 3. The particle size of shale is between 30 nm and 60 μm, and the density is more than 2 g/cm^3, which is beyond the most effective research range of SAS

and connectivity of pores are more accurate (**Figure 5**). Therefore, FIB-SEM is currently the main technical means for studying the three-dimensional structure of shale nanoscale pores (Chalmers et al., 2012; Loucks et al., 2012). Previous authors (Loucks and Reed, 2014; Cheng et al., 2018) analyzed the source of organic pores by the ion polishing–SEM method, and based on this analysis, they further proposed an evolution model of organic pores. The study of organic pores is carried out, the morphology and porosity of different types of organic pores are described in detail, and the geological factors affecting their development are

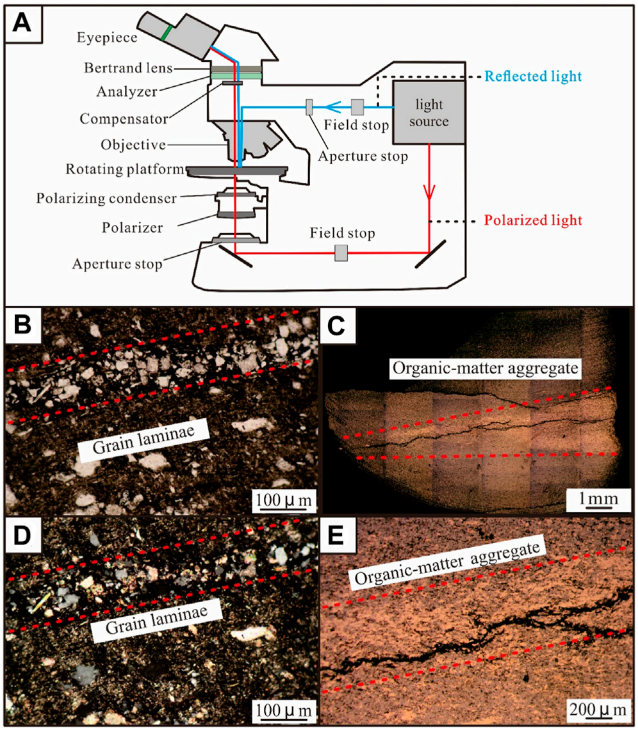

FIGURE 4 | Principle of optical microscope. **(A)** Structure of polarized and reflected light microscopes; **(B)** Grain and crystal lamina in N228-57 (Longmaxi Formation, 3,420.96) at single polarization; **(C)** Stitching picture of reflected light of shale (PS1-06) polished by argon ion; **(D)** Grain laminae in N228-57 at orthogonal polarization; and **(E)** Organic matter aggregate under a reflected light microscope (PS1-06, Longmaxi Formation, 5,957.2 m).

discussed. Using FIB-SEM technology, high-resolution SEM images can be obtained to quantitatively characterize the three-dimensional pore structure of shale at nanoscale. However, due to the limitations of experimental equipment parameters, FIB-SEM demonstrates certain limitations in studying shale porosity and connectivity. Specifically, considering the stability of the ion beam, pores with diameters less than resolution or cutting spacing were not counted, while pores with diameters less than 10 nm were developed in a large number in shale, thereby resulting in porosity results less than the actual value and affecting the calculation and judgment of connectivity (Wang et al., 2018b).

The emergence of AFM technology further improved the resolution to 0.1 nm on the basis of scanning electron microscopy technology. AFM is a scanning probe technology, which, in the early days, was mostly used in biological research. To obtain the topographical structure characteristics of the sample surface, AFM can detect the interaction between samples by measuring the force-sensitive element (**Figure 6**). In this technology, one end of the cantilever arm, which is very sensitive to weak force, is fixed, the colloidal probe at the other end is used to approach the sample to interact, and the repulsive force causes the cantilever arm to be slightly deformed. The small displacement of the cantilever arm is converted into the probe displacement with the help of the principle of optical leverage to obtain the information on the surface topography and roughness of the sample. At present, AFM is widely used in the characterization of shale pores (Cai, 2015), mainly for the observation of pores with a pore diameter of 2–50 nm in shale reservoirs and the study of shale gas storage capacity. Generally speaking, shale samples with lower surface roughness demonstrate smaller specific surface area and poor gas adsorption capacity; shale samples with higher surface roughness demonstrate larger specific surface area and can provide more gas adsorption space (Bai et al., 2016). In addition, AFM is also used to study the wettability of reservoirs. AFM probes can be directly used to measure the thickness of the oil–water film on the surface of the reservoir rock and the force between the material and the liquid film. The degree of characterization can be used to study changes in the wettability of solid surfaces (Wang et al., 2018a).

To form the image, STEM, with a resolution of 0.1–0.2 nm, uses a solid angle scattering generated by the collision of an accelerated concentrated electron beam with a very thin sample. STEM is usually applied to study the crystal structure defects of minerals (Zhang et al., 2012). Previous authors (Bernard et al., 2011; Anderson, 2014) made an attempt to study the nanoscale pore-throat structure of mud shale with different maturity using STEM. They found that organic matter displayed uniform morphological characteristics under SEM, while it showed the different properties under STEM, such as gray scale gradient and energy spectrum characteristics, thus suggesting that multiple types of organic matter exist with different lattice structures in shale, thereby enhancing the understanding of organic matter types and pore evolution of shales. In addition, STEM's penetration imaging features allow three-dimensional micro-nano structures of reservoirs to be characterized (Zhu R. et al., 2016).

Artificial cracks are distinguished in different ways under different equipment. Under an optical microscope, artificial cracks can be distinguished under orthogonal polarized light because they are completely extinct and their height is lower than other minerals. No filler is found in the artificial crack under FIB-SEM, the crack surface is not straight, and no friction mark and fixed direction exist. When scanning the topography under AFM, the crack can be directly observed. It can be judged as artificial cracks according to the fracture, no filling inside, and irregular fracture direction.

3.1.2 Pore, Mineral, and Organic Matter Morphology of Shale Reservoirs

The study of complex pore structures is the key to understanding the mechanism of shale gas accumulation. The pore structure of shale demonstrates a certain particularity due to sedimentation, diagenesis, and geological tectonic transformation (Evdokimov et al., 2006; Bustin et al., 2008). The pore–fracture system in shale includes pores and microfractures, whose pores mainly include organic pores, intragranular pores, and intergranular pores (Loucks et al., 2012; Zhou et al., 2016). Shale is mainly composed of quartz, feldspar, calcite, dolomite, clay minerals, pyrite, and other minerals. Based on the image observation, these

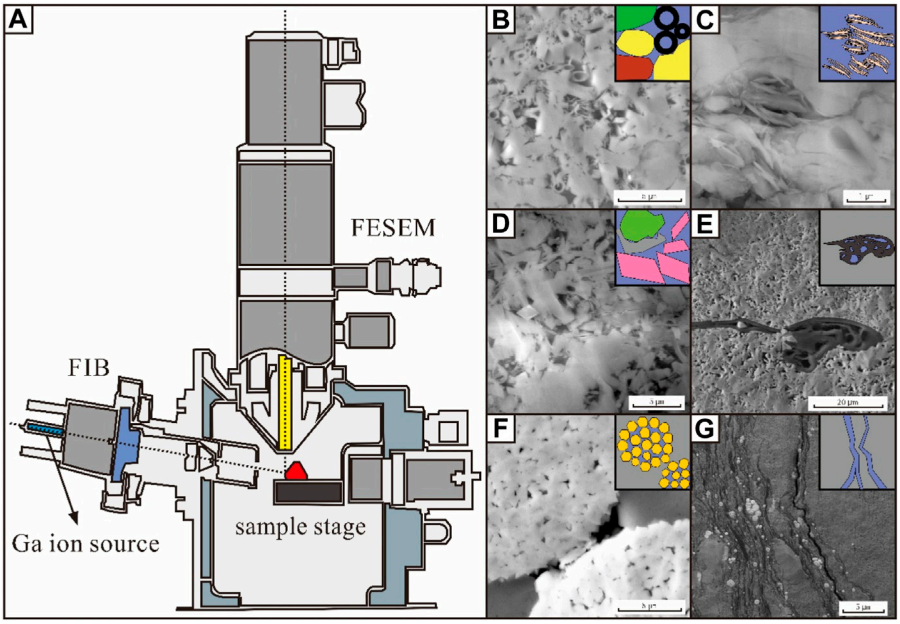

FIGURE 5 | Focused ion beam–scanning electron microscopy (FIB-SEM) structure and the image of shale pore structure: **(A)** Structure of FIB-SEM; **(B)** Intergranular pores and fossil pores; **(C)** Pores between clay platelets; **(D)** Pores between crystals and pores at the edge of rigid grains; **(E)** Organic matter pores; **(F)** Intercrystalline pores within pyrite framboids; and **(G)** Fracture pores (Anderson, 2014).

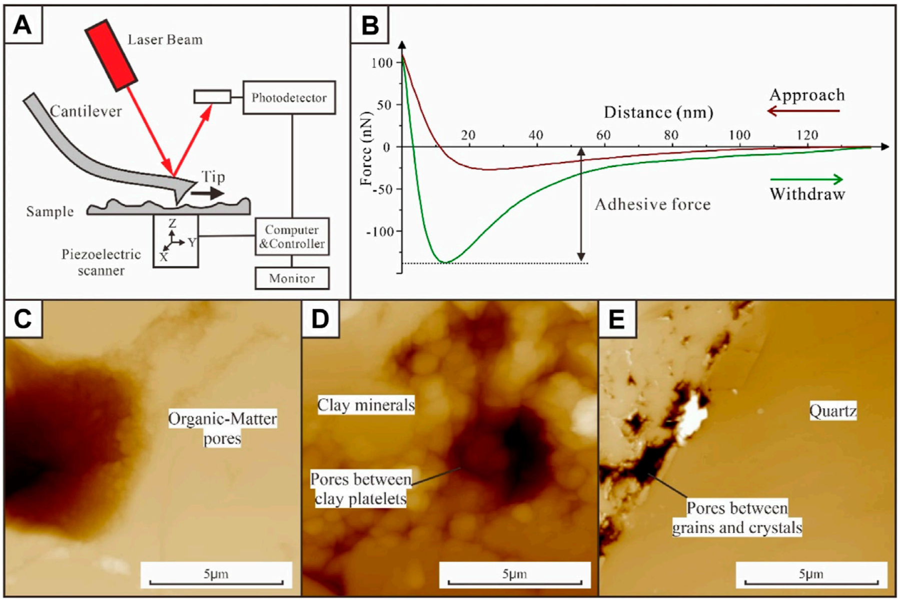

FIGURE 6 | Working principle of atomic force microscopy. **(A)** Experimental principle; **(B)** Schematic curve of force versus distance under the PeakForce QNM mode; **(C)** Organic matter pore morphology of JY4-05 (Wufeng Formation, 2,591.7 m); **(D)** Pore morphology of clay minerals; and **(E)** Intergranular pore morphology.

pores are commonly found in grain laminae and organic matter aggregate (**Table 3**). Next, organic pores are generally round, oval, and irregular in shape, and they are distributed within large continuous organic matter or bitumen filling in the intragranular pores of pyrite framboids. The space of the honeycombed pores extends widely, thereby forming more complex structures and improving pore connectivity. It has been widely accepted that organic pores demonstrate a high degree of development and good connectivity. Mineral pores are relatively few, which are mainly distributed between quartz, feldspar, calcite, and other

TABLE 3 | The type of shale pores and their genetic description.

Shale pore type		Genetic description
Grain laminae	①Pores at the edge of rigid grains ②Moldic pores ③Pores within fossil bodies ④Pores between grains and crystals ⑤Dissolution-rim pores	Boundary pores formed by the compression of rigid grains Pores in shale formed by the dissolution of crystals or fossils A cavity inside a fossil Unfilled pores between crystals and grains during recrystallization or deposition Secondary pores formed by unstable mineral dissolution
Organic matter aggregate	⑥Pores within peloids or pellets ⑦Organic Matter pores ⑧Pores between or within clay platelets ⑨Intercrystalline pores within pyrite framboids	Micropores in biological remains or products related to biological activity Space generated by the shedding of small hydrocarbon molecules in organic matter Interlayer pores formed by the transformation of clay minerals during thermal evolution The unfilled pores left between grains when pyrite accumulates
Fracture	⑩Fracture pores	Pores formed by the dissolution of a soluble mineral by the action of water or gas over a long period

particles or in clay mineral aggregates (Wu et al., 2020b, c; Wu et al., 2019a; Wu et al., 2019c). Microfractures are relatively developed, which are mainly distributed in the boundary between organic matter and minerals, inside brittle minerals, or between clay mineral particles. However, most of them cannot be distinguished as primary fractures formed by the tectonic process or artificial fractures formed during the experimental processes. Organic pores display the characteristics of heterogeneous development due to different types, maturity, and abundance of organic matter, which are manifested as a high degree of development of pores in some places, almost no development of pores in some places, or lower than the instrument resolution (Liu et al., 2019b; Liu et al., 2019c).

3.2 Fluid Injection Techniques and Pore Connectivity in Shale Reservoir

3.2.1 Advantages and Limitations of Fluid Injection Techniques

Fluid injection methods include mercury injection, cryogenic liquid nitrogen adsorption, helium injection, carbon dioxide adsorption, and nuclear magnetic resonance. The mercury injection method can be divided into the conventional (high pressure) mercury injection method and constant-speed mercury injection method, which is mainly used to characterize reservoir pore-throat characteristics and seepage capacity. The conventional mercury injection is to record the amount of injected mercury under a certain pressure to determine the pore structure of rock (**Figure 7**). It demonstrates the characteristics of a wide range of pore sizes, reservoir space (5–995 μm in diameter), and high consistency with the test results of physical properties. However, some errors are found in the measurement of pore throats with a radius less than 50 nm and secondary pore structures with strong diagenesis. Constant-rate mercury injection technology has been widely applied in unconventional reservoir characterization. Pore and throat can be distinguished due to the changing of mercury injection pressure; thus, the size, number, and configuration relationship of pore throat and other reservoir structural characteristics can be quantitatively reflected (Song et al., 2017). However, the pore throat with diameter less than 0.12 μm cannot be generally measured (Zhao et al., 2015). The accuracy of mercury injection in the characterization of pore structure is related to shale physical properties, and it is mostly applicable to shale reservoirs with porosity greater than 5%. A high content of clay minerals and fine pore throat can easily lead to artificial cracks during the analysis, thereby reducing the accuracy (Zhu R. et al., 2016). Therefore, the combination of mercury injection and gas adsorption methods has been widely used to characterize shale reservoir microstructures (Hou et al., 2020).

Low-temperature liquid nitrogen adsorption method is suitable for the characterization of pore volume and specific surface area of micro- and mesopores, which can analyze the structural characteristics of nanopores in shale reservoirs using the adsorption effect of the pore surface on gas and capillary condensation principle, and explore its adsorption capacity and shale gas accumulation power (Gao et al., 2017). Liquid nitrogen condenses and adsorbs on the pore surface, and the thickness of the adsorbed layer thickens with the increase in relative pressure. Next, when the capillary condensation occurs, the adsorption–desorption isotherms of liquid nitrogen on shale can be yielded, thereby obtaining pore-size distribution, volume, and specific surface area (Cao et al., 2015) (**Figure 7**). The disadvantages of low-temperature liquid nitrogen adsorption method include the large measurement error of shale with a small contrast surface area and incomplete pore characterization for a pore size > 100 nm.

Helium injection method uses the characteristics of helium inert gas to calculate the effective pore volume and particle volume of the measured shale according to Boyle's law and obtain shale porosity parameters (**Figure 3D**), which reflect the size of the overall reservoir space of shale, but it is difficult to reflect the distribution of pore throat (Han et al., 2021). Low-pressure CO_2 adsorption technology is often used to analyze pore structure characteristics of < 2 nm, which demonstrates the advantages of short time and fast equilibrium (**Figure 8**). In recent years, numerous authors (Tian et al., 2012; Li T. et al., 2015; Zhu Y. et al., 2016) used low-temperature CO_2 adsorption to study the pore structure characteristics of marine, transitional, and continental shales with different maturities. Researchers

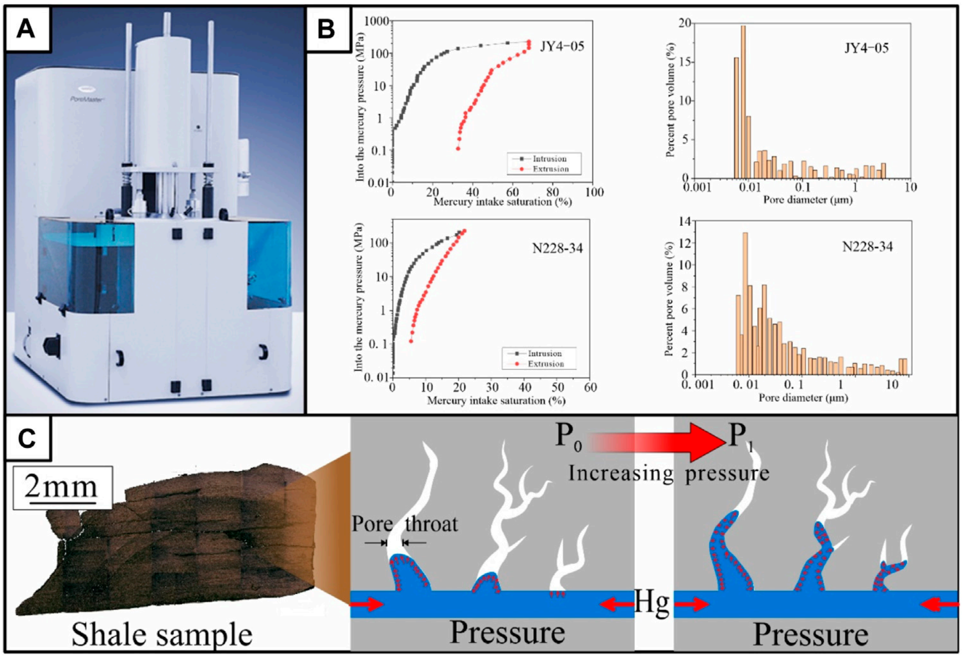

FIGURE 7 | Basic working principle of mercury intrusion porosimetry (MIP). **(A)** Experimental apparatus; **(B)** MIP data curves of different shale samples and its pore distribution characteristics (JY4-05 and N228-34 (Longmaxi Formation, 3,397.87 m)); and **(C)** Schematic diagram of mercury injecting pore throat in massive shale (JY4-09, Longmaxi Formation, 2585.7 m).

found that the low-temperature CO_2 adsorption technology cannot unify the sample processing standard, particle size, pressure boost rate, and other key experimental parameters in the early stage (Tian et al., 2012), and many theoretical models exist for explaining the micropore distribution, but the analysis results differ greatly. The limitations and validity of the total pore space characterization of shale still remain. In addition, three-dimensional characterization methods, like FIB-SEM and Nano-CT, confirmed that the pores less than 2 nm in shale reservoir account for a very small proportion of the reservoir space, and the contribution of these pores to the flow of natural gas and the migration of oil may be very small. Especially, the accuracy of CO_2 adsorption results is usually doubted for the pore structure characterization of shale within the oil window.

Nuclear magnetic resonance (NMR) technology mainly measures the relaxation characteristics of hydrogen-containing fluids in pores using magnetic spectrum and slice imaging (Liu D. et al., 2021), and it obtains the T2 map of relaxation time to characterize the pore size, distribution, connectivity, and fluid occurrence state of shale reservoirs (Ge et al., 2014). NMR images can intuitively obtain information, such as pore and fluid distribution and fracture orientation (Zhou et al., 2012; Huang et al., 2015), but the accuracy of the results is subject to the influence of test environment, fluid properties, and other factors.

According to the experimental principles of various testing methods, the pore sections corresponding to the optimal results are analyzed and superimposed. The pore volume and specific surface area of shale macropores (> 50 nm) are measured using high-pressure mercury intrusion, mesopores (2–50 nm) characterized using low-temperature liquid nitrogen adsorption method, and micropores (< 2 nm) determined by low pressure CO_2 adsorption.

3.2.2 Scaled-Span Pores and the Connectivity in a Shale Reservoir

Shale demonstrates ultra-low porosity and connectivity. The pore-size range is multiscale, thereby accounting for most of the pore volume at the nanoscale. Nanopores in organic matter account for most of the pore volume, which makes shale gas reservoirs demonstrate great methane storage capacity. Slit holes in kerogen were also observed. The spatial distribution of minerals and organic matter is uniform, and most of the pores and throats are isolated with low continuity (Heller and Zoback, 2014).

A large number of previous studies show that abundant microscale and nanoscale pores are found in shales and the pores are mainly ink-bottle organic pores and slits mineral matrix pores. The pore structures of the samples with different total organic content, organic matter type, and mineral compositions showed obvious differences. Organic matter and clay minerals mainly affect the mesopore structure. With the increase in the content of clay minerals and organic matter, the plasticity increases, the ability of shale to resist compaction weakens, and the connectivity of pores worsens (Gao et al., 2017). Next, rigid minerals, such as quartz and carbonate,

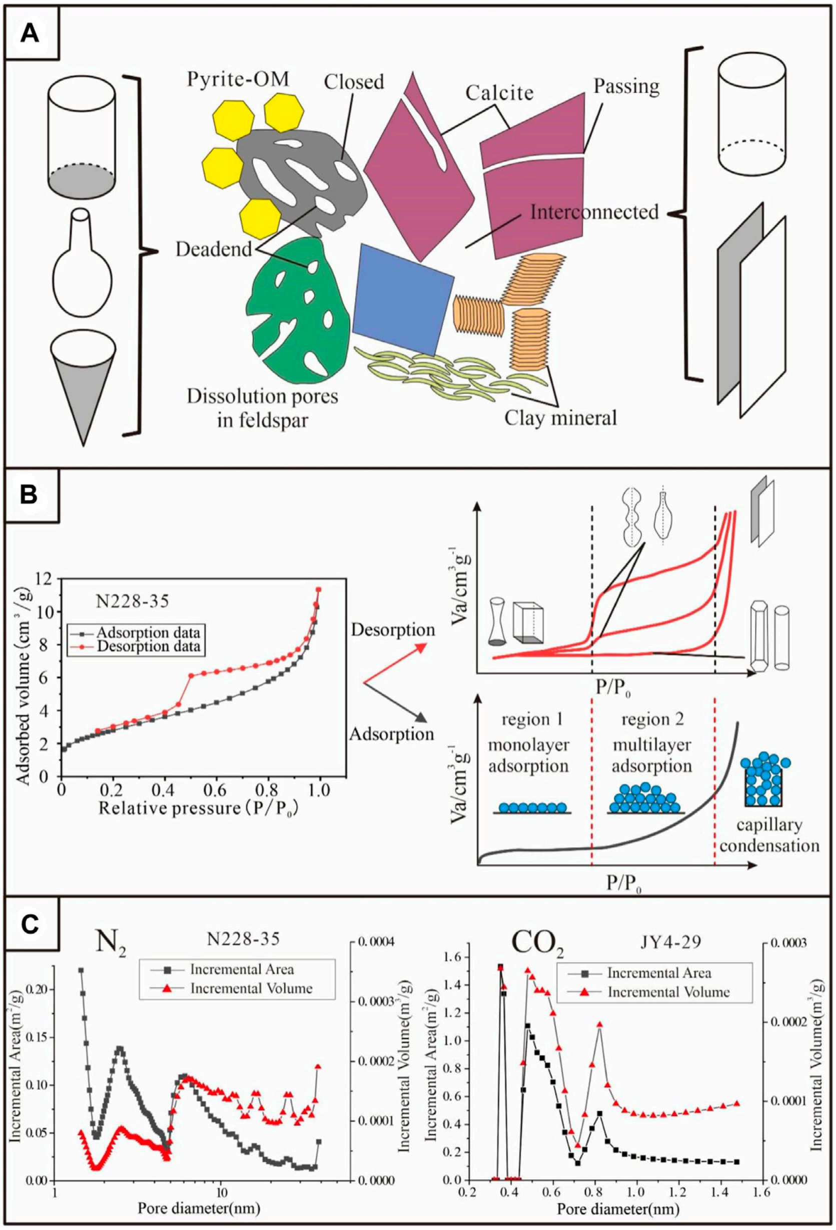

FIGURE 8 | (A) Pore morphology of the organic matter and different minerals in shales (modified from (Nie et al., 2015)); **(B)** Schematic illustration of gas molecules in the whole adsorption process and formation of gas–liquid boundary for different shapes of pores (modified from (Tang et al., 2016; Yin et al., 2019; Ni et al., 2020)); and **(C)** Pore-size distribution curves from N_2 adsorption (N228-35, Longmaxi Formation, 3,398.71 m) and CO_2 adsorption (JY4-29, Longmaxi Formation, 2,548.2 m).

mainly affect the macropore structure, and the retention of intergranular pores can increase the connectivity of pore network.

3.3 High-Energy Ray Techniques and Three-Dimensional Pore Structure

3.3.1 Advantages and Limitations of High-Energy Ray Techniques

High-energy ray method mainly includes small angle scattering and nano/micron CT. A small angle scattering (SAS) can be divided into small angle X-ray scattering (SAXS) and small angle neutron scattering (SANS) according to the source. SAXS originated from the continuous scattering of various submicroscopic particles, such as toner near the incident beam, and its principle is to study the scattering phenomenon of a focused X-ray near the sample. After irradiating it at a very small incident angle, the scattering angle 2θ is smaller than 5° (**Figure 9**). Next, SANS works in a manner similar to SAXS, but it is more sensitive to light elements and demonstrates the identification of isotopes. SAXS/SANS can study the microscopic pore structure and morphological characteristics of shale.

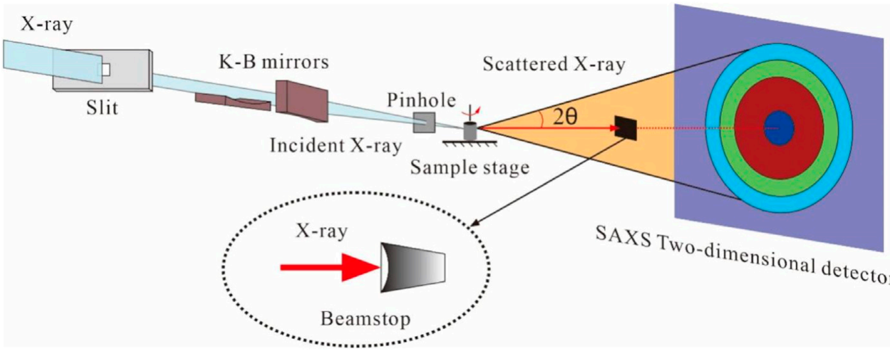

FIGURE 9 | Experimental principle of small angle X-ray scattering.

In shale samples with a relatively simple pore structure and homogeneous composition, the experimental results demonstrate high accuracy and repeatability. In specific reservoir pore characterization, the advantage of SAS is that it can be combined with the fluid injection method to obtain the structural characteristics of closed pores of shales (Zhang et al., 2021). A study on shales of the Longmaxi and Niutitang Formations (Sun et al., 2016; Sun M. et al., 2017) showed that the closed pores were mainly composed of 5–50 nm mesopores, which were related to the pore development within organic matter. Previous studies applied SAS to characterize shale obturator pores (Sun et al., 2016; Sun M. et al., 2017; Sun et al., 2018; Sun et al., 2020). It is believed that high burial depth/maturity reduces the pore connectivity of the shale and increases the content of closed pores. The continuously increasing burial depth compresses the space between mesopores and macropores (Blach et al., 2021), thereby preserving the law of micropore volume. This also means that SAS can effectively characterize the evolution of shale closed pores. On the other hand, in the study of reservoir pore structures, the SAS is still in the initial stage. The main reasons are as follows (Clarkson et al., 2012): 1) the SAS technology is based on a synchrotron radiation platform, and acquiring a synchrotron radiation machine is difficult; 2) a pore structure interpretation model of tight reservoirs, such as shale and tight sandstone, has not yet been formed, which cannot explain the experimental results; and 3) compared with the SAS, the particle diameter of shale reservoir is larger, the particle size is between 30 nm and 60 μm, and the density is more than 2 g/cm^3, which is beyond the most effective research range of SAS.

In a vacuum environment, the X conical wiring harness from the X-ray source on one side of the micro/nano-CT is transmitted to the sample rotating on the sample table and is then received and mapped by the image intensifier on the opposite side (**Figure 10**). The micro/nano-CT technology can characterize the three-dimensional spatial structure of pores, which can be used to evaluate the connectivity of pores. It is mainly based on the density difference, and the gray difference is often used to distinguish different components. For shales, the intensity range can be assigned by interactive threshold processing to characterize pores, organic matter, matrix minerals, and high-density minerals in turn. The connectivity of the pore–fracture network in shales can be simulated using the ball-and-stick model of imaging. Previous works (Guo et al., 2016; He et al., 2016) showed that pyrite in shales, such as the Longmaxi Formation, is randomly distributed on the basis of nano-CT scanning and three-dimensional reconstruction technology, and it is mainly displays elliptic and berry spherical shapes, with particle sizes ranging from several hundred nanometers to dozens of microns. Other mineral components rarely display obvious granularity, which are formed by mutual compaction and mixing. Most of the organic matter was irregularly connected, and the total volume was approximately 5%. The pores and fractures are mostly distributed in organic matter and between different minerals, and most of them are ellipsoid, with strong heterogeneity of pore volume and a significant difference in pore connectivity.

3.3.2 Three-Dimensional Pore Structure and its Impact on Gas Occurrence in Shale Reservoir

The effect of shale pore structure on gas adsorption and seepage is to establish gas flow models based on an FIB-SEM image, nano-CT image, or micron CT image. Gas flow models in shale mainly include the continuum model, discrete fracture network model, and mixed model. The continuous media model gradually developed into the dual media model, triple media model, quadruple media model, etc. Its advantage is that different seepage media have been considered separately, which can better reflect the actual situation. With the increasing complexity of the model, however, the difficulty of solving the model increases sharply. The discrete fracture model is more consistent with the flow law of the actual fluid in the reservoir, but it is difficult to divide the grid and obtain the parameters. The hybrid model fully combines the advantages of a continuum model and discrete fracture model, but it still demonstrates some problems, such as complex modeling, low computational efficiency, and inadequate applicability to faults and complex boundaries when describing seepage channels at different scales (Ozkan et al., 2010; Freeman et al., 2011; Sun H. et al., 2017; Li Z. et al., 2019).

Previous studies have shown that adsorbed gas was mainly stored in pore spaces of less than 10 nm, and free gas mainly existed in pores of more than 50 nm (Ambrose et al., 2010). The

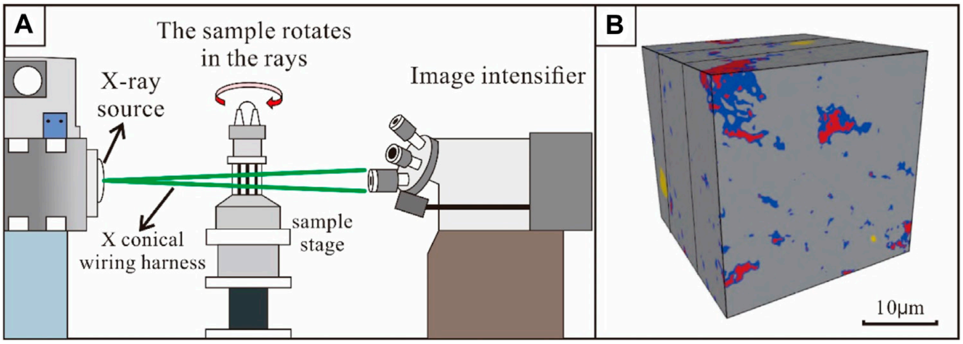

FIGURE 10 | Basic work principle of micro-computed tomography (CT). **(A)** Experimental principle; **(B)** 3D reconstruction of shale cores under CT (Gou et al., 2019).

law of gas migration in large pores is described by the Stokes equation, while the law of gas migration in micropores is described by the Darcy equation. The methane gas in macropores is desorbed faster, which accelerates the movement of methane gas in the whole system. Continuous growth of micropores can significantly enhance the overall connectivity of porous media and contribute significantly to the shale gas flow process (Huang and Zhao, 2017; Li Z. et al., 2019).

When the pore pressure is low, the ratio of the apparent permeability to the Darcy permeability is high, and the influence of temperature and gas molar mass is reduced. Knudsen diffusion is an important gas migration process in the shale system. The diffusion contribution is greater in smaller pores, lower pressures and temperatures, and at higher molar mass gases (Javadpour, 2009; Freeman et al., 2011; Sun H. et al., 2017).

Using the three-dimensional structure established by FIB-SEM or CT, pore volume, pore surface area, porosity, and connectivity can be calculated. Studies displayed that the pore surface area and pore volume were highly correlated with the gas content (Cai et al., 2013; Cai et al., 2018; Liu D. et al., 2021; Liu Z. et al., 2021). Researchers observed that microporosity can make the surface of the pore space rougher and increase the connectivity of the pore space (Li J. et al., 2015; Wu et al., 2019a; Wu et al., 2019b), which causes an increase in permeability as the absolute permeability of the pore space increases. The pore network analysis of predecessors revealed that micropores demonstrate a significant impact on pore and throat distributions, especially the throat, since most micropores act primarily as throats (Wu et al., 2019a).

4 CONCLUSION

Research on shale gas reservoirs has made continuous progress, but many challenges remain. To improve the effectiveness of marine, marine-continental transitional, and continental shale gas exploration and development, it is necessary to sort out and summarize the composition and spatial configuration of shale gas reservoirs and establish simplified models and evaluation standards based on the analysis system. In this article, the microscopic characteristics of shale reservoirs and the differences, advantages, and disadvantages of research techniques are systematically sorted out, and some ideas for the characterization of cross-scale pore networks are sorted out. The main conclusions are as follows:

1) A simplified model of the microstructure of shale can be established based on the laminae structure. Shale consists of grain laminae, organic matter aggregate, and fracture. Grain laminae is mainly composed of inorganic pores, which provide less specific surface area and contribute a certain rigidity to the whole rock. Organic matter aggregate is composed of organic matter, clay minerals, and pyrite symbiosis, which is a relatively plastic layer and a well-porous layer of shale. The fracture enhances the internal seepage capacity of the reservoir.
2) The microstructure analysis techniques of shale reservoirs can be classified into three categories: image observation method, fluid injection method, and high-energy ray method. The image observation method mainly studies the pore type, size, and distribution by means of direct observation. The fluid injection method uses indirect testing as a means to quantitatively analyze the size of the reservoir space. The high-energy ray method is an indirect analysis method, and the key technology is repeatability. It can mainly quantitatively analyze the shape, size, and distribution characteristics of the closed storage space.
3) For generally homogeneous material, the single structure and composition indicate that the local microscopic phenomenon is representative of the whole. Shale is a heterogeneous rock material, and the representation of microscopic phenomena to the whole sample becomes poor with the decreasing observation scales. Therefore, when we use the existing technology to study the microstructure of shales, it is necessary to connect with the paleosedimentary environment and use the macroscopic constraints on the research methods of microscopic features without exaggerating the role of microscopic features.

AUTHOR CONTRIBUTIONS

YQ and PG designed research; YQ and YC performed research; YQ, FS, and XF draw the pictures; and YQ and YZ wrote the article.

FUNDING

This work was funded by the National Natural Science Foundation of China (Grant nos. U19B6003-03-01 and 42030804).

REFERENCES

Ambrose, R. J., Hartman, R. C., Diaz-Campos, M., Akkutlu, I. Y., and Sondergeld, C. H. (2010). "New Pore-Scale Considerations for Shale Gas in Place Calculations," in SPE unconventional gas conference (Pittsburgh, PA: OnePetro).

Anderson, T. (2014). *Key Parameters for Liquid-Rich Unconventional Plays: Case Studies from North America. AAPG Search Discov*. Canada, 33. Article 80354.

Bai, Y., Liu, M., Yang, C., and Jiang, Z. (2016). AFM Based Pore Characterization of Shales and its Relation to the. *Anal. Gas J. Jilin Univ. (Earth Sci. Ed.* 46, 1332–1341.

Bernard, S., Horsfield, B., Schulz, H.-M., Schreiber, A., and Wirth, R. (2011). *Gas Generation Reactions in Highly Mature Gas Shales*. Houston, TX: Search and Discovery, 80162.

Blach, T., Radlinski, A. P., Vu, P., Ji, Y., de Campo, L., Gilbert, E. P., et al. (2021). Accessibility of Pores to Methane in New Albany Shale Samples of Varying Maturity Determined Using SANS and USANS. *Energies* 14, 8438. doi:10.3390/en14248438

Bustin, R. M., Bustin, A. M., Cui, A., Ross, D., and Pathi, V. M. (2008). "Impact of Shale Properties on Pore Structure and Storage Characteristics," in SPE shale gas production conference (Fort Worth, TX: OnePetro).

Cai, X. (2015). Application of Atomic Force Microscopy in the Study of Microscopic Pore Structure of Shale. *J. Chin. Electron Microsc. Soc.* 34, 326–331.

Cai, Y., Li, Q., Liu, D., Zhou, Y., and Lv, D. (2018). Insights into Matrix Compressibility of Coals by Mercury Intrusion Porosimetry and N2 Adsorption. *Int. J. Coal Geol.* 200, 199–212. doi:10.1016/j.coal.2018.11.007

Cai, Y., Liu, D., Pan, Z., Yao, Y., Li, J., and Qiu, Y. (2013). Pore Structure and its Impact on CH4 Adsorption Capacity and Flow Capability of Bituminous and Subbituminous Coals from Northeast China. *Fuel* 103, 258–268. doi:10.1016/j.fuel.2012.06.055

Campbell, C. V. (1967). Lamina, Laminaset, Bed and Bedset. *Sedimentology* 8, 7–26. doi:10.1111/j.1365-3091.1967.tb01301.x

Cao, G., Wang, L., Zhang, Y., and Yang, Z. (2015). Research on Nitrogen Physical Adsorption Method and Mercury Intrusion Method Used for Characterization of FCC Catalyst Pore Size. *distribution Refin. Chem. Industry* 26, 9–12.

Chalmers, G. R., Bustin, R. M., and Power, I. M. (2012). Characterization of Gas Shale Pore Systems by Porosimetry, Pycnometry, Surface Area, and Field Emission Scanning Electron Microscopy/transmission Electron Microscopy Image Analyses: Examples from the Barnett, Woodford, Haynesville, Marcellus, and Doig Units. *Bulletin* 96, 1099–1119. doi:10.1306/10171111052

Cheng, Z., Xue, H., Li, W., Lu, S., and Zhou, N. (2018). Quantitative Characterization of Reservoir Space of Tight Sandstones Based on a Large-View FE-SEM Splicing Technology: a Case Study on the Hetaoyuan Formation in Biyang Sag. *China Pet. Explor.* 23, 79–87.

Clarkson, C. R., Freeman, M., He, L., Agamalian, M., Melnichenko, Y. B., Mastalerz, M., et al. (2012). Characterization of Tight Gas Reservoir Pore Structure Using USANS/SANS and Gas Adsorption Analysis. *Fuel* 95, 371–385. doi:10.1016/j.fuel.2011.12.010

Curtis, J. B. (2002). Fractured Shale-Gas Systems. *AAPG Bull.* 86, 1921–1938. doi:10.1306/61eeddbe-173e-11d7-8645000102c1865d

Curtis, M. E., Ambrose, R. J., Sondergeld, C. H., and Rai, C. S. (2011). "Transmission and Scanning Electron Microscopy Investigation of Pore Connectivity of Gas Shales on the Nanoscale," in North American unconventional gas conference and exhibition (The Woodlands, TX: OnePetro).

Evdokimov, I. N., Eliseev, N. Y., Losev, A. P., and Novikov, M. A. (2006). "Emerging Petroleum-Oriented Nanotechnologies for Reservoir Engineering," in SPE Russian oil and gas technical conference and exhibition (Moscow, Russia: OnePetro). doi:10.2118/102060-RU

Freeman, C. M., Moridis, G. J., and Blasingame, T. A. (2011). A Numerical Study of Microscale Flow Behavior in Tight Gas and Shale Gas Reservoir Systems. *Transp. Porous Med.* 90, 253–268. doi:10.1007/s11242-011-9761-6

Gao, F., Song, Y., Jiang, Z., Zhang, X., and Chen, L. (2017). Influence of Clay Minerals on Shale Storage Space and Adsorptive Capacity Special Oil and Gas Reservoirs. *ACS Omega* 24, 1–8.

Ge, X., Fan, Y., Zhu, X., Chen, Y., and Li, R. (2014). Determination of Nuclear Magnetic Resonance T2 Cutoff Value Based on Multifractal Theory — an Application in Sandstone with Complex Pore Structure. *Geophysics* 80, D11–D21.

Gou, Q., Xu, S., Hao, F., Yang, F., Wang, Y., Lu, Y., et al. (2019). Study on Characterization of Micro-fracture of Shale Based on Micro-CT. *Acta Geol. Sin.* 93, 2372–2382. doi:10.1111/1755-6724.14154

Guo, X., He, S., Chen, S., Chen, X., Wang, S., and Qin, L. (2016). Research on Microstructure of Shale Pores and Distribution Features Based on. *Nano-CT Scanning Digital Core Analysis Coal Geol. China* 28, 28–34.

Han, X., Zhang, H., Mao, X., and Xu, D. (2021). A Method of Gas Porosity Measurement for Tight Reservoirs Based on Mechanical Analysis of Core Chamer Chinese. *J. Geophys.* 64, 287–297.

He, Z., Nie, H., and Zhang, Y. (2016). The Main Factors of Shale Gas Enrichment of Ordovician Wufeng Formation-Silurian Longmaxi Formation in the Sichuan Basin and its Adjacent Areas Earth. *Sci. Front.* 23, 8–17.

Heller, R., and Zoback, M. (2014). Adsorption of Methane and Carbon Dioxide on Gas Shale and Pure Mineral Samples. *J. Unconv. oil gas Resour.* 8, 14–24. doi:10.1016/j.juogr.2014.06.001

Hou, H., Shao, L., Tang, Y., Zhao, S., Yuan, Y., Li, Y., et al. (2020). Quantitative Characterization of Low-Rank Coal Reservoirs in the Southern Junggar Basin, NW China: Implications for Pore Structure Evolution Around the First Coalification Jump. *Mar. Petroleum Geol.* 113, 104165. doi:10.1016/j.marpetgeo.2019.104165

Huang, J., Xu, K., Guo, S., and Guo, H. (2015). Comprehensive Study on Pore Structures of Shale Reservoirs Based on SEM, NMR and X-CT. *Geoscience* 29, 198–205.

Huang, X., and Zhao, Y.-P. (2017). Characterization of Pore Structure, Gas Adsorption, and Spontaneous Imbibition in Shale Gas Reservoirs. *J. Petroleum Sci. Eng.* 159, 197–204. doi:10.1016/j.petrol.2017.09.010

Ingram, R. L. (1954). Terminology for the Thickness of Stratification and Parting Units in Sedimentary Rocks. *Geol. Soc. Am. Bull.* 65, 937–938. doi:10.1130/0016-7606(1954)65[937:tfttos]2.0.co;2

Javadpour, F. (2009). Nanopores and Apparent Permeability of Gas Flow in Mudrocks (Shales and Siltstone). *J. Can. Petroleum Technol.* 48, 16–21. doi:10.2118/09-08-16-da

Lai, J., Wang, G., Wang, Z., Chen, J., Pang, X., Wang, S., et al. (2018). A Review on Pore Structure Characterization in Tight Sandstones. *Earth-Science Rev.* 177, 436–457. doi:10.1016/j.earscirev.2017.12.003

Lazar, O. R., Bohacs, K. M., Macquaker, J. H. S., Schieber, J., and Demko, T. M. (2015). Capturing Key Attributes of Fine-Grained Sedimentary Rocks in Outcrops, Cores, and Thin Sections: Nomenclature and Description Guidelines. *J. Sediment. Res.* 85, 230–246. doi:10.2110/jsr.2015.11

Lei, Y., Luo, X., Wang, X., Zhang, L., Jiang, C., Yang, W., et al. (2015). Characteristics of Silty Laminae in Zhangjiatan Shale of Southeastern Ordos Basin, China: Implications for Shale Gas Formation. *Bulletin* 99, 661–687. doi:10.1306/09301414059

Li, C., Xiao, Q., Chen, Q., and Jiang, X. (2019a). Evolution Characteristics and Controls of Shale Nanopores during Thermal Maturation of Organic Matter. *Pet. Geol. & Exp.* 41, 901–909.

Li, J., Yin, J., Zhang, Y., Lu, S., Wang, W., Li, J., et al. (2015a). A Comparison of Experimental Methods for Describing Shale Pore Features - A Case Study in the Bohai Bay Basin of Eastern China. *Int. J. Coal Geol.* 152, 39–49. doi:10.1016/j.coal.2015.10.009

Li, T., Tian, H., Chen, J., and Cheng, L. (2015b). The Application of Low Pressure Gas Adsorption to the Characterization of Pore Size Distribution for Shales: An Example from Southeastern Chongqing Area. *Nat. Gas. Geosci.* 26, 1719–1728.

Li, Z., Yan, W., Qi, Z., Dong, D., Huang, X., and Yu, R. (2019b). Production Performance Model Based on Quadruple-Porosity Medium in Shale Gas Reservoirs Considering Multi-Transport Mechanisms. *Energy Sources, Part A Recovery, Util. Environ. Eff.*, 1–19. doi:10.1080/15567036.2019.1662520

Liu, D., Zou, Z., Cai, Y., Qiu, Y., Zhou, Y., and He, S. (2021a). An Updated Study on CH4 Isothermal Adsorption and Isosteric Adsorption Heat Behaviors of Variable Rank Coals. *J. Nat. Gas Sci. Eng.* 89, 103899. doi:10.1016/j.jngse.2021.103899

Liu, G., Huang, Z., Chen, F., Jiang, Z., Gao, X., Li, T., et al. (2016a). Reservoir Characterization of Chang 7 Member Shale: A Case Study of Lacustrine Shale in the Yanchang Formation, Ordos Basin, China. *J. Nat. Gas Sci. Eng.* 34, 458–471. doi:10.1016/j.jngse.2016.06.071

Liu, G., Huang, Z., Jiang, Z., Chen, J., Chen, F., and Xing, J. (2016b). Gas Adsorption Capacity Calculation Limitation Due to Methane Adsorption in Low Thermal Maturity Shale: A Case Study from the Yanchang Formation, Ordos Basin. *J. Nat. Gas Sci. Eng.* 30, 106–118. doi:10.1016/j.jngse.2016.01.026

Liu, G., Zhai, G., Huang, Z., Zou, C., Xia, X., Shi, D., et al. (2019a). The Effect of Tuffaceous Material on Characteristics of Different Lithofacies: A Case Study on Lucaogou Formation Fine-Grained Sedimentary Rocks in Santanghu Basin. *J. Petroleum Sci. Eng.* 179, 355–377. doi:10.1016/j.petrol.2019.04.072

Liu, G., Zhai, G., Yang, R., He, T., and Wei, B. (2021b). Quartz Crystallinity Index: New Quantitative Evidence for Biogenic Silica of the Late Ordovician to Early Silurian Organic-Rich Shale in the Sichuan Basin and Adjacent Areas, China. *Sci. China Earth Sci.* 64, 773–787. doi:10.1007/s11430-020-9718-2

Liu, G., Zhai, G., Zou, C., Cheng, L., Guo, X., Xia, X., et al. (2019b). A Comparative Discussion of the Evidence for Biogenic Silica in Wufeng-Longmaxi Siliceous Shale Reservoir in the Sichuan Basin, China. *Mar. Petroleum Geol.* 109, 70–87. doi:10.1016/j.marpetgeo.2019.06.016

Liu, G., Zhai, G., Zou, C., Huang, Z., Liu, B., Guo, X., et al. (2019c). Amorphous Silica and its Effects on Shale Reservoir: A Case Study about Yanchang Formation Lacustrine Shale, Ordos Basin. *Energy Sources, Part A Recovery, Util. Environ. Eff.* 41, 975–989. doi:10.1080/15567036.2018.1522395

Liu, Z., Liu, D., Cai, Y., and Qiu, Y. (2021c). Permeability, Mineral and Pore Characteristics of Coals Response to Acid Treatment by NMR and QEMSCAN: Insights into Acid Sensitivity Mechanism. *J. Petroleum Sci. Eng.* 198, 108205. doi:10.1016/j.petrol.2020.108205

Loucks, R. G., Reed, R. M., Ruppel, S. C., and Hammes, U. (2012). Spectrum of Pore Types and Networks in Mudrocks and a Descriptive Classification for Matrix-Related Mudrock Pores. *Bulletin* 96, 1071–1098. doi:10.1306/08171111061

Loucks, R. G., and Reed, R. M. (2014). Scanning-electron-microscope Petrographic Evidence for Distinguishing Organic-Matter Pores Associated with Depositional Organic Matter versus Migrated Organic Matter in Mudrock. *Gulf Coast Assoc. Geol. Soc. J.* 3, 51–60.

Ni, G., Li, S., Rahman, S., Xun, M., Wang, H., Xu, Y., et al. (2020). Effect of Nitric Acid on the Pore Structure and Fractal Characteristics of Coal Based on the Low-Temperature Nitrogen Adsorption Method. *Powder Technol.* 367, 506–516. doi:10.1016/j.powtec.2020.04.011

Nie, B., Liu, X., Yang, L., Meng, J., and Li, X. (2015). Pore Structure Characterization of Different Rank Coals Using Gas Adsorption and Scanning Electron Microscopy. *Fuel* 158, 908–917. doi:10.1016/j.fuel.2015.06.050

Ozkan, E., Raghavan, R., and Apaydin, O. G. (2010). "Modeling of Fluid Transfer from Shale Matrix to Fracture Network," in SPE Annual Technical Conference and Exhibition (Florence, Italy: OnePetro).

Peltonen, C., Marcussen, Ø., Bjørlykke, K., and Jahren, J. (2009). Clay Mineral Diagenesis and Quartz Cementation in Mudstones: The Effects of Smectite to Illite Reaction on Rock Properties. *Mar. Petroleum Geol.* 26, 887–898. doi:10.1016/j.marpetgeo.2008.01.021

Peng, Li., Ting, D., and Nicholas, B. H. (2014). *Microstructural Characterization of Gas Shales by Electron Microscopy*. Calgary, AB: AAPG Search Discov. Article 90224.

Qiu, Z., and Zou, C. (2020). Controlling Factors on the Formation and Distribution of "Sweet-Spot Areas" of Marine Gas Shales in South China and a Preliminary Discussion on Unconventional Petroleum Sedimentology. *J. Asian Earth Sci.* 194, 103989. doi:10.1016/j.jseaes.2019.103989

Ross, D. J. K., and Marc Bustin, R. (2009). The Importance of Shale Composition and Pore Structure upon Gas Storage Potential of Shale Gas Reservoirs. *Mar. petroleum Geol.* 26, 916–927. doi:10.1016/j.marpetgeo.2008.06.004

Sang, Q., Zhao, X., Liu, Y., Li, Z., and Dong, M. (2022). Effects of the Laminated-Structure and Mixed Wettability on the Oil/water Relative Permeabilities and Oil Productions in Shale Oil Formations. *J. Petroleum Sci. Eng.* 208, 109457. doi:10.1016/j.petrol.2021.109457

Shi, C., Cao, J., Tan, X., Luo, B., Zeng, W., Hong, H., et al. (2018). Hydrocarbon Generation Capability of Sinian-Lower Cambrian Shale, Mudstone, and Carbonate Rocks in the Sichuan Basin, Southwestern China: Implications for Contributions to the Giant Sinian Dengying Natural Gas Accumulation. *Bulletin* 102, 817–853. doi:10.1306/0711171417417019

Song, L., Ning, Z., Sun, Y., Ding, G., and Du, H. (2017). Pore Structure Characterization of Tight Oil Reservoirs by a Combined Mercury Method Petroleum Geology. *Experiment* 39, 700–705.

Sun, H., Yao, J., Cao, Y.-c., Fan, D.-y., and Zhang, L. (2017a). Characterization of Gas Transport Behaviors in Shale Gas and Tight Gas Reservoirs by Digital Rock Analysis. *Int. J. Heat Mass Transf.* 104, 227–239. doi:10.1016/j.ijheatmasstransfer.2016.07.083

Sun, J., Yang, Z., Liu, X., and Xiong, S. (2012). Reservoir Wettability Evaluation Using Nuclear Magnetic Resonance Technology. *Sci. Technol. Rev.* 30, 65–71.

Sun, M., Yu, B., Hu, Q., Chen, S., Xia, W., and Ye, R. (2016). Nanoscale Pore Characteristics of the Lower Cambrian Niutitang Formation Shale: A Case Study from Well Yuke #1 in the Southeast of Chongqing, China. *Int. J. Coal Geol.* 154-155, 16–29. doi:10.1016/j.coal.2015.11.015

Sun, M., Yu, B., Hu, Q., Yang, R., Zhang, Y., Li, B., et al. (2018). Pore Structure Characterization of Organic-Rich Niutitang Shale from China: Small Angle Neutron Scattering (SANS) Study. *Int. J. Coal Geol.* 186, 115–125. doi:10.1016/j.coal.2017.12.006

Sun, M., Yu, B., Hu, Q., Zhang, Y., Li, B., Yang, R., et al. (2017b). Pore Characteristics of Longmaxi Shale Gas Reservoir in the Northwest of Guizhou, China: Investigations Using Small-Angle Neutron Scattering (SANS), Helium Pycnometry, and Gas Sorption Isotherm. *Int. J. Coal Geol.* 171, 61–68. doi:10.1016/j.coal.2016.12.004

Sun, M., Zhang, L., Hu, Q., Pan, Z., Yu, B., Sun, L., et al. (2020). Multiscale Connectivity Characterization of Marine Shales in Southern China by Fluid Intrusion, Small-Angle Neutron Scattering (SANS), and FIB-SEM. *Mar. Petroleum Geol.* 112, 104101. doi:10.1016/j.marpetgeo.2019.104101

Tang, X., Ripepi, N., Stadie, N. P., Yu, L., and Hall, M. R. (2016). A Dual-Site Langmuir Equation for Accurate Estimation of High Pressure Deep Shale Gas Resources. *Fuel* 185, 10–17. doi:10.1016/j.fuel.2016.07.088

Tian, H., Zhang, S., Liu, S., and Zhang, H. (2012). Determination of Organic-Rich Shale Pore Features by Mercury Injection and Gas Adsorption Methods. *Acta Pet. Sin.* 33, 419–427.

Wang, Y., Bai, Y., Hou, B., Wang, R., Bai, Q., and Zhang, X. (2018a). Mechanistic Study on Wettability Alteration of Oil-Wet Sandstone Surface Using Mixed Cationic-Nonionic Surfactants. *J. China Univ. Petroleum* 42, 165–171.

Wang, Y., Wang, L., Wang, J., and Jiang, Z. (2018b). Three-dimension Characterization of Organic Matter Pore Structures of Shale Using Focused Ion Beam-Scanning Electron Microscope. *Rock Mineral Analysis* 37, 235–243.

Wu, Y., Lin, C., Yan, W., Liu, Q., Zhao, P., and Ren, L. (2020a). Pore-scale Simulations of Electrical and Elastic Properties of Shale Samples Based on Multicomponent and Multiscale Digital Rocks. *Mar. Petroleum Geol.* 117, 104369. doi:10.1016/j.marpetgeo.2020.104369

Wu, Y., Tahmasebi, P., Lin, C., and Dong, C. (2020b). A Comprehensive Investigation of the Effects of Organic-Matter Pores on Shale Properties: A Multicomponent and Multiscale Modeling. *J. Nat. Gas Sci. Eng.* 81, 103425. doi:10.1016/j.jngse.2020.103425

Wu, Y., Tahmasebi, P., Lin, C., and Dong, C. (2020c). Process-based and Dynamic 2D Modeling of Shale Samples: Considering the Geology and Pore-System Evolution. *Int. J. Coal Geol.* 218, 103368. doi:10.1016/j.coal.2019.103368

Wu, Y., Tahmasebi, P., Lin, C., Munawar, M. J., and Cnudde, V. (2019a). Effects of Micropores on Geometric, Topological and Transport Properties of Pore Systems for Low-Permeability Porous Media. *J. Hydrology* 575, 327–342. doi:10.1016/j.jhydrol.2019.05.014

Wu, Y., Tahmasebi, P., Lin, C., Ren, L., and Dong, C. (2019b). Multiscale Modeling of Shale Samples Based on Low- and High-Resolution Images. *Mar. Petroleum Geol.* 109, 9–21. doi:10.1016/j.marpetgeo.2019.06.006

Wu, Y., Tahmasebi, P., Lin, C., Zahid, M. A., Dong, C., Golab, A. N., et al. (2019c). A Comprehensive Study on Geometric, Topological and Fractal Characterizations of Pore Systems in Low-Permeability Reservoirs Based on SEM, MICP, NMR, and X-Ray CT Experiments. *Mar. Petroleum Geol.* 103, 12–28. doi:10.1016/j.marpetgeo.2019.02.003

Xiao, X.-M., Wei, Q., Gai, H.-F., Li, T.-F., Wang, M.-L., Pan, L., et al. (2015). Main Controlling Factors and Enrichment Area Evaluation of Shale Gas of the Lower Paleozoic Marine Strata in South China. *Pet. Sci.* 12, 573–586. doi:10.1007/s12182-015-0057-2

Yang, B., Xiong, M., Chen, L., and Huang, D. (2020). Laminae Growth Characteristic within the Lower Silurian Longmaxi Marine Shale in the Southeast Sichuan Basin. *Adv. Geosciences* 10, 555–562.

Yin, T., Liu, D., Cai, Y., and Zhou, Y. (2019). Methane Adsorption Constrained by Pore Structure in High-Rank Coals Using FESEM, CO2 Adsorption, and NMRC Techniques. *Energy Sci. Eng.* 7, 255–271. doi:10.1002/ese3.275

Zhang, J., Hu, C., Yao, C., and Fang, W. (2012). Determination of Microstructure and Defect Structure in Pyrophyllite by High- Resolution Transmission Electron Microscopy. *Acta Mineral. Sin.* 32, 65–73.

Zhang, L., Xu, Y., Sun, M., and Jiang, S. (2021). The Structure and Evolution of Closed Pores in Shale Determined by Small Angle Neutron Scattering. *Acta Sedimentol. Sin.* 39, 310–323.

Zhao, H., Ning, Z., Wang, Q., Zhang, R., Zhao, T., Niu, T., et al. (2015). Petrophysical Characterization of Tight Oil Reservoirs Using Pressure-Controlled Porosimetry Combined with Rate-Controlled Porosimetry. *Fuel* 154, 233–242. doi:10.1016/j.fuel.2015.03.085

Zhou, K., Li, J., Xu, Y., and Zhang, Y. (2012). Measurement of Rock Pore Structure Based on NMR Technology. *J. Central South Univ. Sci. Technol.* 43, 4796–4800.

Zhou, S., Yan, G., Xue, H., Guo, W., and Li, X. (2016). 2D and 3D Nanopore Characterization of Gas Shale in Longmaxi Formation Based on FIB-SEM. *Mar. Petroleum Geol.* 73, 174–180. doi:10.1016/j.marpetgeo.2016.02.033

Zhu, R., Wu, S., Su, L., and Cui, J. (2016a). Problems and Future Works of Porous Texture Characterization of Tight Reservoirs in China. *Acta Pet. Sin.* 37, 1323–1336.

Zhu, Y., Wang, Y., Chen, S., and Zhang, H. (2016b). Qualitative-quantitative Multiscale Characterization of Pore Structures in Shale Reservoirs: A Case Study of Longmaxi Formation in the Upper Yangtze Area. *Earth Sci. Front.* 23, 154–163.

Zou, C., Dong, D., Wang, Y., Li, X., and Huang, J. (2015). Shale Gas in China: Characteristics, Challenges and Prospects (I). *Petroleum Explor. Dev.* 42, 689–701. doi:10.1016/s1876-3804(15)30072-0

Zou, C., Zhao, Q., Cong, L., Wang, H., Shi, Z., Wu, J., et al. (2021). Development Progress, Potential and Prospect of Shale Gas in China. *Nat. Gas. Ind.* 41, 1–14.

Zou, C., Zhao, Q., Dong, D., Yang, Z., Qiu, Z., and Liang, F. (2017). Geological Characteristics,main Challenges and Future Prospect of Shale Gas. *Nat. Gas. Geosci.* 28, 1781–1796. doi:10.1016/j.jnggs.2017.11.002

Conflict of Interest: The authors declare that the research was conducted in the absence of any commercial or financial relationships that could be construed as a potential conflict of interest.

Publisher's Note: All claims expressed in this article are solely those of the authors and do not necessarily represent those of their affiliated organizations or those of the publisher, the editors, and the reviewers. Any product that may be evaluated in this article or claim that may be made by its manufacturer is not guaranteed or endorsed by the publisher.